Fidelity Maps for Model Update under Uncertainty: Application to a Piano Soundboard

Sylvain Lacaze* and Samy Missoum†

Aerospace and Mechanical Engineering Department, University of Arizona, Tucson, Arizona, 85721

This paper presents a new approach for model updating based on fidelity maps. Fidelity maps are used to explicitly define regions of the random variable space within which the discrepancy between computational and experimental data is below a threshold value. It is shown that fidelity maps, built as a function of epistemic and aleatory uncertainties, can be used to calculate the likelihood for maximum likelihood estimates or Bayesian update. The fidelity map approach has the advantage of handling numerous correlated responses at a moderate computational cost. This is made possible by the use of an adaptive sampling scheme to build accurate boundaries of the fidelity maps. Although the proposed technique is general, it is specialized to the case of model update for modal properties (natural frequencies and mode shapes). A simple plate and a piano soundboard finite element model with uncertainties on the boundary conditions are used to demonstrate the methodology.

I. Introduction

Computational models are used to predict the behavior of systems and minimize the use of experimental testing. However, because of assumptions on boundary conditions, material properties etc., the computational model rarely matches the experimental data. For this reason, the model must be modified (or "updated" or "tuned") to obtain a satisfactory agreement. For instance, in computational modal analysis, the objective is often to match natural frequencies and mode shapes obtained from experimental testing.[1–3] Because uncertainties might have a pronounced effect on the response of the system, their inclusion in the update process is now recognized as a necessity.

Until rather recently, model update was mostly associated with the deterministic minimization of the difference, often in a least-square sense, between computational and experimental data. This is particularly true in the field of modal analysis. The corresponding "one point solution" might be highly sensitive to uncertainties with, as a consequence, a poor predictive capability. For this reason, statistical approaches have been used to extract distributions of update parameters and responses. The two most common statistical approaches are the maximum likelihood and Bayesian update. While the maximum likelihood approach[4,5] finds the most "probable" values of the parameters to be estimated, the Bayesian method[6,7] focuses on refining the parameter distributions inferred from previous knowledge. In any case, both approaches require the construction of a likelihood function.

Several difficulties are hampering the construction of an accurate likelihood in the general case. The hurdles are due to the large computational costs associated with modern simulation techniques, the large number of responses to be matched as well as their correlation and the presence of discontinuities. In addition, the construction of the likelihood should be made with as fewer assumptions as possible. However, in the literature, many studies are based on, for instance, assumptions on the form of the error distributions.[1,3]

The proposed update approach is designed to provide a flexible scheme which tackles the aforementioned technical difficulties such as the inclusion of correlated responses or the computational time. This work is based on the construction of explicit boundaries of the domain of the parameters space where the discrepancy

*Graduate Student, AME Department and AIAA Student Member.

†Associate Professor, AME Department and AIAA Senior Member.

between model and experiments is below a given threshold. This domain with the corresponding boundaries are referred to as "fidelity maps". The boundaries are constructed using a support vector machine (SVM) which is a classification technique used to explicitly separate data belonging to two classes.[8–11] The use of a classification technique has the advantage of allowing the inclusion of a large number of responses used for the update. In addition, the correlation between the responses is implicitly accounted for.

The fidelity maps are built in a space of random variables that correspond to aleatory and epistemic uncertainties. Some of the variables corresponding to epistemic uncertainties can be chosen to be estimated. As an example, the fidelity map can be built in the space with a random load (aleatory uncertainty) and a material property (epistemic uncertainty) that one wants to estimate. An accurate boundary can be created using an adaptive sampling scheme developed by the authors.[12–14] Once the boundary is obtained, a likelihood can be constructed by generating Monte-Carlo samples for the aleatory variables. Once the likelihood is constructed, parameters that need to be estimated can be found by maximizing the likelihood. It can also be used for Bayesian update.

Although the proposed methodology is general, this article focuses on model update from modal testing. In particular, this study considers the comparison of computational and experimental natural frequencies and mode shapes. The mode shapes are compared using a modal assurance criterion (MAC) matrix whose handling is made simpler with the fidelity maps. The focus application is the update of a finite element model of a piano soundboard.

This article is constructed as follows. Section II provides a background on model updating where Section II.E will focus on model updating from modal testing and describing the various quantities used. Section III will describe the calculation of the likelihood for a given fidelity map. Section III.A provides a background on SVM and Section III.C on the adaptive sampling to accurately build the SVM. Finally, Section IV will present results related to a demonstrative plate example and to the piano soundboard. Both examples include uncertainties on the boundary conditions.

II. Background

Consider a measurement y^{exp}. A model is available (e.g., a Finite Element model), with an output y which should approximate y^{exp}. The model uses two kinds of input parameters. First, the parameters that need to be identified. This work refers to it as *epistemic* parameters, noted $\mathbf{e}$, even so it could be just a subset of all epistemic uncertainties of the model. Second, the parameters that cannot be controlled, with irreducible uncertainties, referred to as the *aleatory* ones, noted $\mathbf{a}$. In a same fashion it could be only a subset of all aleatory uncertainties of the model. The actual, unknown, values of the parameters to estimate are noted $\mathbf{e}_{act}$. The Probability density function (PDF) of a random variable X is noted $\mathbf{f}_X$ and its cumulative distribution function (CDF) is noted $\mathbf{F}_X$. For a vector of random variables we use bold notation (e.g. $\mathbf{x}$) and we refer to its i^{th} component as x_i.

II.A. Least Square Estimate

The Least Square Approach, and its more evolved derivation, the Generalized Least Square,[15] is the mostly used and simplest approach for model update. This approach is purely deterministic as it does not include uncertainties. A typical least square formulation is:

$$\mathbf{e_{est}} = \underset{\mathbf{e}}{\mathbf{argmin}}\ J(\mathbf{e}, \mathbf{a}^\star) \tag{1}$$

with:

$$J(\mathbf{e}, \mathbf{a}^\star) = \sum_{i=1}^{n_m} (y_i^{exp} - y_i(\mathbf{e}, \mathbf{a}^\star))^2 \tag{2}$$

where n_m is the dimension of the measurement vector. In the classic formulation, $\mathbf{a}^\star$ would not appear, as the approach is purely deterministic and $\mathbf{A}$ represents stochastic quantities. However, it is possible to introduce some uncertainties, by setting the stochastic quantities $\mathbf{A}$ to user defined deterministic value $\mathbf{a}^\star$. These values are obtained through expert knowledge or experience, classically the mean of the random variables, the median or the most probable value. This approach has been shown to present limitations mostly when the model outputs are correlated, of different magnitude or different dispersions.[2] In order to mitigate this issue and include uncertainties, the likelihood[4,5] is introduced as described in the following subsection.

II.B. Maximum Likelihood Estimate

A common approach to perform identification or model update is to use Maximum Likelihood Estimate (MLE). This approach can be seen as half-deterministic, half-stochastic as random input can be used but a single point results on the estimated parameters. This quantity is defined as the probability density that $\mathbf{y} = \mathbf{y^{exp}}$ for a given $\mathbf{e}$. By maximizing it, the estimates are the ones that make the model outputs most likely to be equal to the measurements. Therefore we can express the likelihood of a given $\mathbf{e}$ as the conditional joint probability density function (PDF) $\mathbf{f_{Y(E,A)|E=e}(y^{exp})}$. Consequently, a possible MLE formulation is:

$$\mathbf{e_{est}} = \underset{\mathbf{e}}{\mathbf{argmax}}\ \mathbf{f_{Y(E,A)|E=e}(y^{exp})} \tag{3}$$

We can observe that the model output is now stochastic as the variability on $\mathbf{A}$ is taken into account and propagated through the model. The core of this approach lies into being able to compute an accurate joint conditional PDF. This point is detailed in Section III.B.

As mentioned previously, this approach provides a point estimate of $\mathbf{e_{est}}$. In order to obtain a distribution of $\mathbf{e_{est}}$ and have a fully stochastic approach, one can use the Bayesian approach.

II.C. Bayesian Approach

The Bayesian inference theory[6,7] provides a way to derive a stochastic estimate based on stochastic inputs. This approach is based on the Bayes formula:

$$\mathbf{f}_{A|B}\mathbf{f}_B = \mathbf{f}_{B|A}\mathbf{f}_A \tag{4}$$

Specializing the Bayes formula to our problem, we have:

$$\mathbf{f_{E|Y(E,A)}f_{Y(E,A)}} = \mathbf{f_{Y(E,A)|E}f_E} \tag{5}$$

Which can be rewritten as:

$$\mathbf{f_{E|Y(E,A)}} = \frac{\mathbf{f_{Y(E,A)|E}f_E}}{\mathbf{f_{Y(E,A)}}} \tag{6}$$

This is the functional expression, therefore, for a given set of epistemic parameters $\mathbf{e}$ and a given set of measurement $\mathbf{y^{exp}}$:

$$\mathbf{f_{E|Y(E,A)=y^{exp}}(e)} = \frac{\mathbf{f_{Y(E,A)|E=e}(y^{exp})f_E(e)}}{\mathbf{f_{Y(E,A)}(y^{exp})}} \tag{7}$$

where:

- $\mathbf{f_E(e)}$ is called the *prior*. This corresponds to the existing knowledge on the distribution of the $\mathbf{E}$.
- $\mathbf{f_{E|Y(E,A)=y^{exp}}(e)}$ is called the *posterior*. It is the updated distribution of parameters to estimate based on the prior knowledge and a set of measurements $\mathbf{y^{exp}}$;
- $\mathbf{f_{Y(E,A)|E=e}(y^{exp})}$ is the likelihood;
- $\mathbf{f_{Y(E,A)}(y^{exp})}$ is actually a simple normalizing constant which could be obtained by propagating all uncertainties through the model. The latter being in most cases impossible to do, the use of techniques such as Markov Chain Monte Carlo (MCMC) simulations[16–18] allows one to circumvent this difficulty.

II.D. Scientific Challenges

The Bayesian approach and Maximum Likelihood have their own sets of challenges. The Bayesian approach hinges on the availability of an accurate prior knowledge. Although it is not always possible, this mainly involves expert knowledge, available data (e.g. for material properties) or quantification techniques (e.g. Maximum Entropy principle[19]). In addition, the Bayesian approach requires the ability to sample the posterior. This is traditionally done with MCMC[16–18] which comes with its own set of hurdles (e.g, if the posterior distribution is multi-modal[3]). Both the MLE and Bayesian approaches require the calculation of the likelihood which is made difficult by the following points:

- Possibly correlated measurements;
- Numerous measurements;
- Possibly binary or discontinuous responses;
- Computationally intensive model;
- Exact analytical expression of the likelihood cannot be expressed.

The proposed work lies the foundation for an approach that mitigate the consequences of these hurdles.

II.E. Finite element Model updating based on modal data

The proposed methodology in this paper will be applied to the Finite Element Model (FEM) update for modal data (e.g., natural frequencies and mode shapes). This is a typical application of model updating with specific quantities used to compare model and experimental data:[20,21]

- Differences in natural frequencies values (e.g., Euclidean norm of difference). This quantity is traditionally minimized in the form of a residual through optimization. Various weights can be assigned to the different frequencies if more emphasis is to be given to particular ones.
- Differences between the mode shapes. This is typically measured using the Modal Assurance Criterion (MAC) matrix (see below).
- Differences between the Frequency Response Function (FRFs) measured using the FRAC (Frequency Response Assurance Criterion).
- Mode orthogonality.

The "MAC" criterion is by far the most widely used:

$$MAC_{ij} = \frac{(\Phi_i^{*T} A \Phi_{exp,j})^2}{(\Phi_i^{*T} A \Phi_i)(\Phi_{exp,j}^{*T} A \Phi_{exp,j})} \tag{8}$$

where Φ_i is the i^{th} computational mode shape and "*exp*" stands for experimental. Φ_i^{*T} is the conjugate transpose of the mode shape. *It is essential to use the conjugate of the mode shape if the modes are complex.* A is often the identity matrix or the mass matrix. For N modes, the MAC values can be gathered in a matrix as depicted in Figure 1. The MAC value is equal to unity for a perfect match of modes. It should be as close to zero as possible for cross terms.

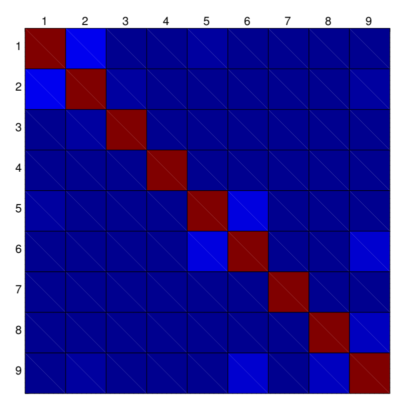

Figure 1: Example of MAC matrix with 9 modes. The matrix quantifies the match between experimental and computational mode shapes. A perfect match would have 1 (red) on the diagonal and 0 (blue) for cross terms.

III. Fidelity maps and construction of the likelihood

The main concept of the proposed approach lies in the identification of regions of the space of random variables within which the error between the model and the experiments is below a given threshold ε. The boundaries of these regions, referred to as fidelity maps, are constructed explicitly using a Support Vector Machine (SVM). Once the boundaries are created, it can be shown (see Section III.B) that the likelihood can be obtained efficiently. This main idea is depicted on Figure 2. The main advantages of the fidelity map approach stems from the fact that no assumption needs to be made on the form of the likelihood, that it can handle a large number of correlated responses, and , secondarily, it can tackle problems with discontinuities. In addition, an adaptive sampling scheme allows to reduce the number of function evaluations.

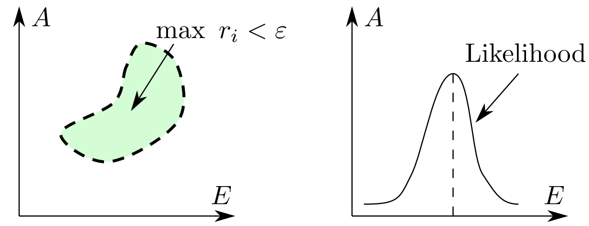

Figure 2: Main idea of the fidelity map: define explicitly the regions of the space of random variables within which the the model matches the experiments with an accuracy ε.

III.A. SVM-based fidelity map

A Support Vector Machine (SVM) is a classifier that is able to define boundaries between samples of two different classes (e.g, feasible and infeasible).[8–11] Being a classification method, its main advantage stems from the fact that it can handle discontinuous and binary data.[12] SVM can produce highly nonlinear boundaries corresponding to non-convex and disjoint regions. Given N training sample, the SVM classifier is expressed as:

$$s(\mathbf{x}) = b + \sum_{k=1}^{N} \lambda^{(k)} l^{(k)} K(\mathbf{x}^{(k)}, \mathbf{x}) \tag{9}$$

where $\mathbf{x}^{(k)}$ is the k^{th} training sample, $\lambda^{(k)}$ is the corresponding Lagrange multiplier, $l^{(k)}$ is the label (class) that can take values +1 or -1, K is a kernel function and b is the bias. The boundary is then defined for $s(\mathbf{x}) = 0$. The prediction of the class of any point $\mathbf{x}$ is given by the sign of $s(\mathbf{x})$. The Lagrange multipliers $\lambda^{(k)}$ are strictly positive for the *support vectors* and zero for all other samples, which implies that the SVM is entirely defined by the support vectors. Regarding the kernel K, several choices are available, such as polynomial kernel and Gaussian kernel. In this work, we use a Gaussian kernel defined as:

$$K(\mathbf{x}^{(k)}, \mathbf{x}) = e^{-\gamma ||\mathbf{x}^{(k)} - \mathbf{x}||^2} \quad , \quad \gamma > 0 \tag{10}$$

In order to build the fidelity maps, an SVM is initially trained using a design of experiments (DOE). The class of each sample is defined based on the discrepancy between the model outputs and the experimental "measurements". To be feasible, a training sample must correspond to absolute relative differences between the model outputs y_i and the measurements y_i^{exp} less than a given threshold. In the general case, one could set different thresholds ε_i for all the outputs. Therefore, the labels used to train the SVM are defined as:

$$l^{(k)} = \begin{cases} +1 & \text{if } \forall i \; r_i^{(k)} \leq \varepsilon_i \\ -1 & \text{otherwise} \end{cases} \qquad \text{where} \qquad r_i^{(k)} = \left| \frac{y_i^{(k)} - y_i^{exp}}{y_i^{exp}} \right| \tag{11}$$

III.B. Likelihood computation

Given a fidelity map and a set of parameters to identify, it can be shown that as the ε_i tend to zero, the likelihood can be obtained. This can be proven, without loss of generality and for the sake of simplicity, with e and y^{exp} as two scalars. The relation between a PDF and a CDF is given as:

$$\mathbf{f}_{Y(E,\mathbf{A})|E=e}(y^{exp}) = \frac{\mathrm{d}\mathbf{F}_{Y(E,\mathbf{A})|E=e}}{\mathrm{d}y}(y^{exp}) \tag{12}$$

Using central finite differences, we have:

$$\mathbf{f}_{Y(E,\mathbf{A})|E=e}(y^{exp}) = \lim_{\varepsilon \to 0} \frac{\mathbf{F}_{Y(E,\mathbf{A})|E=e}(y^{exp}+\varepsilon) - \mathbf{F}_{Y(E,\mathbf{A})|E=e}(y^{exp}-\varepsilon)}{2\varepsilon} \tag{13}$$

Recall that $\mathbf{F}_X(x) = P[X < x]$, which leads to $\mathbf{F}_X(x^{(1)}) - \mathbf{F}_X(x^{(2)}) = P[x^{(2)} < X < x^{(1)}]$. It is then possible to rewrite (13) as:

$$\mathbf{f}_{Y(E,\mathbf{A})|E=e}(y^{exp}) = \lim_{\varepsilon \to 0} \frac{\mathbf{P}_{E=e}[Y(E,\mathbf{A}) \leq y^{exp}+\varepsilon] - \mathbf{P}_{E=e}[Y(E,\mathbf{A}) \leq y^{exp}-\varepsilon]}{2\varepsilon} \tag{14}$$

$$\mathbf{f}_{Y(E,\mathbf{A})|E=e}(y^{exp}) = \lim_{\varepsilon \to 0} \frac{\mathbf{P}_{E=e}[y^{exp}-\varepsilon \leq Y(E,\mathbf{A}) \leq y^{exp}+\varepsilon]}{2\varepsilon} \tag{15}$$

The probability $\mathbf{P}_{Y(E,\mathbf{A})|E=e}[y^{exp}-\varepsilon \leq Y \leq y^{exp}+\varepsilon]$ represents the probability of a given e to generate outputs lying into the "feasible region" of the fidelity map and can be efficiently estimated using Monte Carlo Sampling over the aleatory variables. As ε tends to zero, this probability tends to the likelihood value. The idea is illustrated on Figure 3 in one dimension. A MLE can then be obtained through the use of an optimization algorithm. As this works aim to demonstrate the general idea, in Section IV, the MLEs are obtained by brute forcely computing the likelihood at a given number of set $\mathbf{e}$ and taking the maximum of these values.

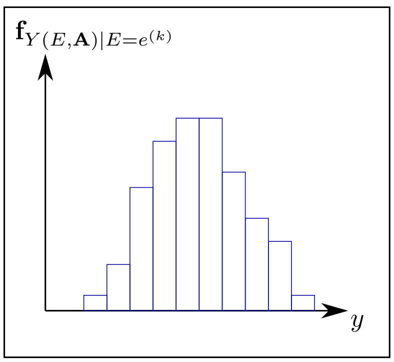

(a) For $e^{(k)}$, propagate the uncertainties through y, due to $\mathbf{A}$.

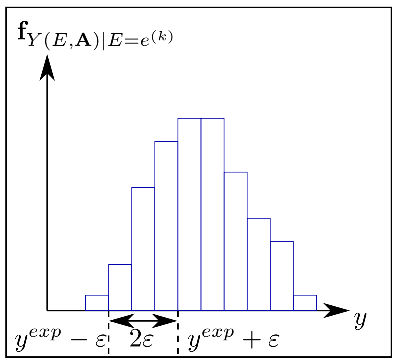

(b) Compute the ratio of points falling into the range of 2ε.

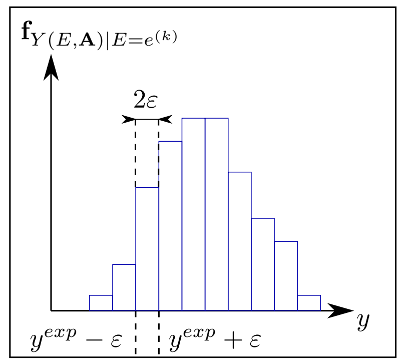

(c) As ε tend to zero, this ratio actually becomes the likelihood value, up to a constant of 2ε.

Figure 3: Illustration of likelihood computation using Monte Carlo Sampling as ε tend to zeros.

III.C. Map refinement and adaptive sampling

In order for the likelihood to be accurate, a small enough ε is needed as well as an accurate boundary.

III.C.1. Ensure at least one "feasible" sample

It might happen that while following the initial DOE, there is not a single sample that satisfies the initial fidelity requirement imposed by the various (small) ε_i. Therefore no feasible sample is available to construct an SVM. In order to solve this issue, the sample $\mathbf{x}^{(k_c)}$ with the minimum discrepancy over all the responses is searched and assigned a +1 label. The index k_c is:

$$k_c = \arg\min_k \quad r_{max}^{(k)} \quad \text{where} \quad r_{max}^{(k)} = \max_i \left(\frac{r_i^{(k)}}{\varepsilon_i} - 1 \right) \tag{16}$$

III.C.2. Adaptive sampling

In order to build an accurate SVM at affordable cost, Basudhar et al.[13,14] introduced an adaptive sampling scheme that is used in this work. Algorithm 1 describes how the labels are defined during the adaptive sampling scheme.

Algorithm 1 Fidelity map. Adaptive Sampling.

Require: User define how small the fidelity map must be by setting $\boldsymbol{\varepsilon}$;

Sample the space (composed of $\mathbf{e} \cup \mathbf{a}$) according to a DOE of size n (here, CVT) : $\mathbf{x}^{(k)} = [\mathbf{e}^{(k)}, \mathbf{a}^{(k)}]$;

Evaluate all samples : $\mathbf{y}^{(k)} = \mathbf{y}(\mathbf{x}^{(k)})$;

Define the scaled residual relative to each measurements for all points : $r_i^{(k)} = \left| \frac{y_i^{exp} - y_i^{(k)}}{y_i^{exp}} \right|$;

For each point, define their "feasibility" : $r_{max}^{(k)} = \max\limits_i \left(\frac{r_i^{(k)}}{\varepsilon_i} - 1 \right)$;

for $j = n+1 \to n + n_{adapt}$ **do** ; Begin adaptive sampling

  Set all labels to -1: $l^{(k)} = -1 \; \forall k$;

  Define $\mathbb{K} = \left\{ k_i | r_{max}^{(k_i)} \leq 0 \right\}$ and set $l^{(k_i)} = +1 \quad k_i \in \mathbb{K}$;

  if $\mathbb{K} = \varnothing$ **then**;

    Find $k_c = \arg\min\limits_l r_{max}^{(l)}$ and set $l^{(k_c)} = +1$;

  end if

  Build the SVM as explained in Section III.A;

  Add an adaptive sample $\mathbf{x}^{(j)}$ as explain in Section III.C.2;

  Compute : $\mathbf{y}^{(j)}, \mathbf{r}^{(j)}, r_{max}^{(j)}$;

end for

Two types of samples are used in the EDSD adaptive sampling process:[13,14]

A primary sample is used to refine the boundary. Also referred as "maxmin" sample, it is defined as the point in the space that maximizes the minimum distance to existing samples under the constraint that it lies on the SVM boundary (i.e., $s(\mathbf{x})$=0).

A secondary sample is used to prevent a phenomenon referred as "locking" of the SVM, where adding primary samples only generates small changes of the boundary. For this reason, this sample is also referred to as 'anti-locking' sample.

The schedule used in this work is two primary samples and one secondary sample. More details related to the primary and secondary samples are provided in Appendix A.

IV. Results

The proposed methodology is applied to two FE model update problems. It is first applied to a simple plate problem with uncertainty on the boundary condition and for which the Young's modulus needs to be identified. The approach is then applied to a piano soundboard with uncertainties on the boundary conditions, and the material properties. For comparison purposes, the results are performed along with an approach based on a residual as well as the product of the likelihoods corresponding to the various responses (See Appendix B). Although the product of likelihoods is usually used for problems with independent measurements error, it is used here to show how it behaves on correlated model outputs. The residual used in the examples is defined as:

$$R = \sum_{i=1}^{N} \left[\frac{(\lambda_i - \lambda_i^{exp})^2}{\lambda_i^{exp}} + (MAC_{ii} - 1)^2 + \sum_{j=1, j \neq i}^{N} MAC_{ij} \right] \tag{17}$$

Note that the the residual is based on relative differences as opposed to absolute differences, which is what is traditionally done.

IV.A. Simple Plate

As a first example, we consider a rectangular plate. The plate is simply supported. In order to model the uncertainties in the displacement boundary conditions, one dimensional springs of stiffness K are used for three sides of the plate (Figure 4). The finite element model of the plate is constructed with 80 shell elements. We wish to identify the Young's modulus E of the plate. The parameters are summarized in Table 1. In order to define "experiments" the FE model is run with $E = E_{act}$ and $K = K_{act}$. All the examples are run with $\varepsilon = 1\%$ for all the responses. The identification of E is based on the first four modes.

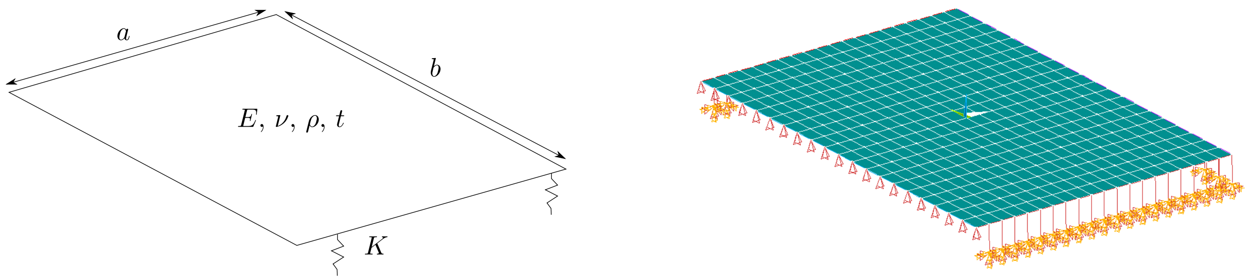

(a) Schematic representation. (b) FEM representation

Figure 4: Schematic and Finite Element representation of a simple plate. One side is simply supported while the others are connected to the ground through springs, to model uncertainties on the boundary conditions.

Table 1: Parameters used for the plate example (S.I. units).

	Deterministic					Epistemic	Aleatory
Parameter	a	b	ν	ρ	t	E	K
Value, Distribution	1	1.5	0.33	7800	0.01	N/A	$U(2 \times 10^5, 10^6)$

The fidelity map is constructed in the (E, K) space with 15 Central Voronoi Tesselation (CVT) samples. The boundary is then refined with 50 additional adaptive samples. The likelihood is then constructed for different values of E (one dimensional problem). For each value of E, the probability of being within the fidelity map is calculated with 10^5 Monte Carlo samples according to the distribution of K. This provide a conditional probability, which, for small values of ε is the likelihood, noted LH_{mcs}. The value of E corresponding to the maximum likelihood can then be obtained.

The proposed approach is compared to the results using the likelihood of the residual (LH_{res}) and the product of the likelihoods for the different responses LH_{prod} (see Appendix B). These likelihoods are constructed using Kriging models[22–25] trained with 65 CVT samples and Kernel Smoothing.[26]

The three likelihoods are constructed based on 6 combinations of E_{act} and K_{act} (see Table 2). The results are depicted on Figures 5 and 6.

Table 2: Summary of the 6 experimental combinations and Figures associated (S.I. units).

E_{act}	185×10^9			235×10^9		
K_{act}	3×10^5	6×10^5	9×10^5	3×10^5	6×10^5	9×10^5
Figures	5a & 5b	5c & 5d	5e & 5f	6a & 6b	6c & 6d	6e & 6f

It is clear that LH_{mcs} show a higher robustness than the two other methods for that example. The failure of the LH_{prod} is obvious since the different natural frequencies are strongly correlated, therefore, the assumption of independence leads to incorrect results. The inability for LH_{res} to reach the maximum is not straightforward. A loose explanation stems from the gathering of several responses within one quantities that are correlated and might have different spreads.

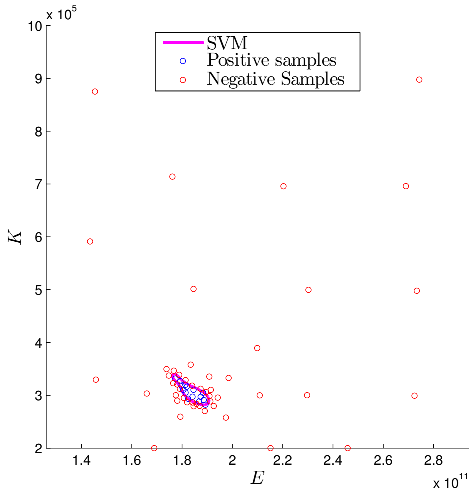

(a) SVM process

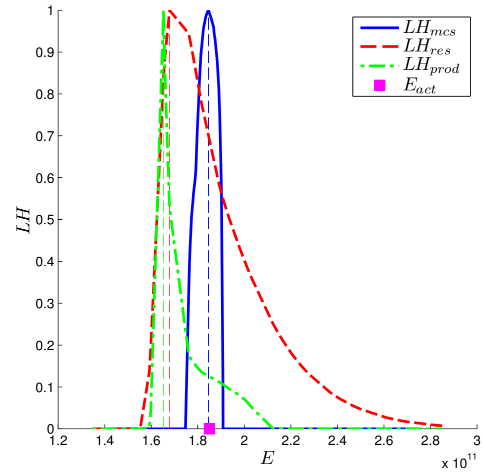

(b) Likelihood

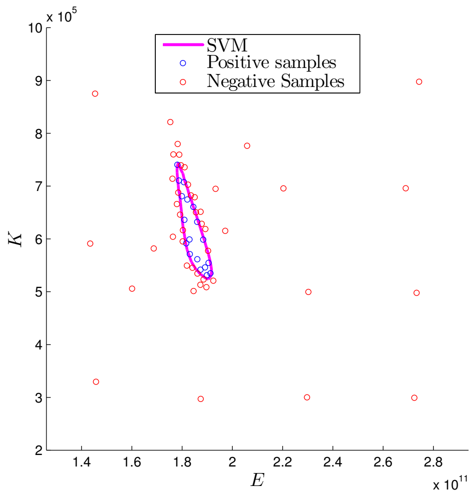

(c) SVM process

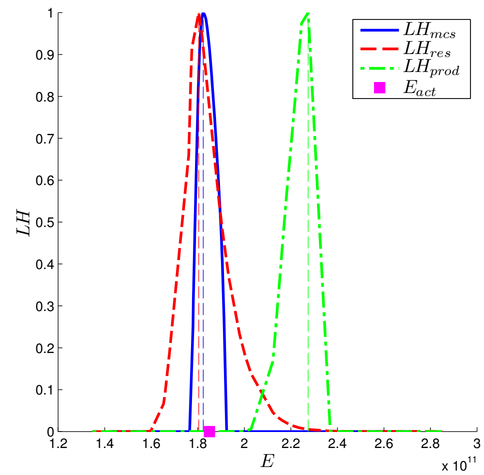

(d) Likelihood

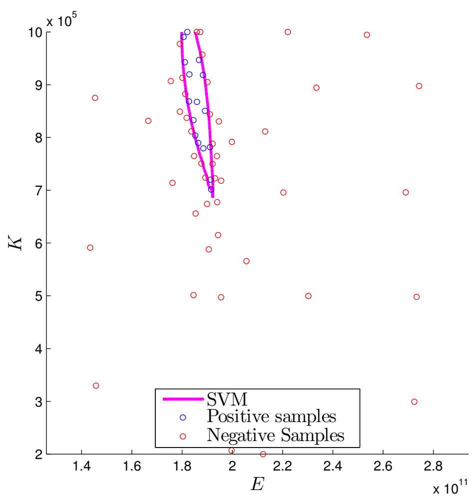

(e) SVM process

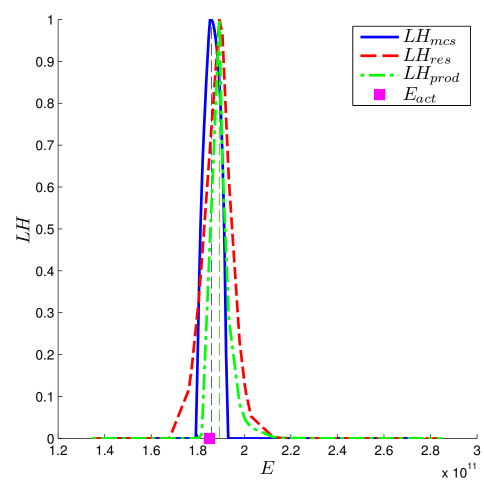

(f) Likelihood

Figure 5: Results of the plate example for $E_{act} = 185 \times 10^9\ Pa$ and $K_{act} = 3 \times 10^5\ N.m^{-1}$ (a and b), $K_{act} = 6 \times 10^5\ N.m^{-1}$ (c and d) and $K_{act} = 9 \times 10^5\ N.m^{-1}$ (e and f). The figures on the left show the final SVM while the ones on the right show the likelihoods (S.I. units).

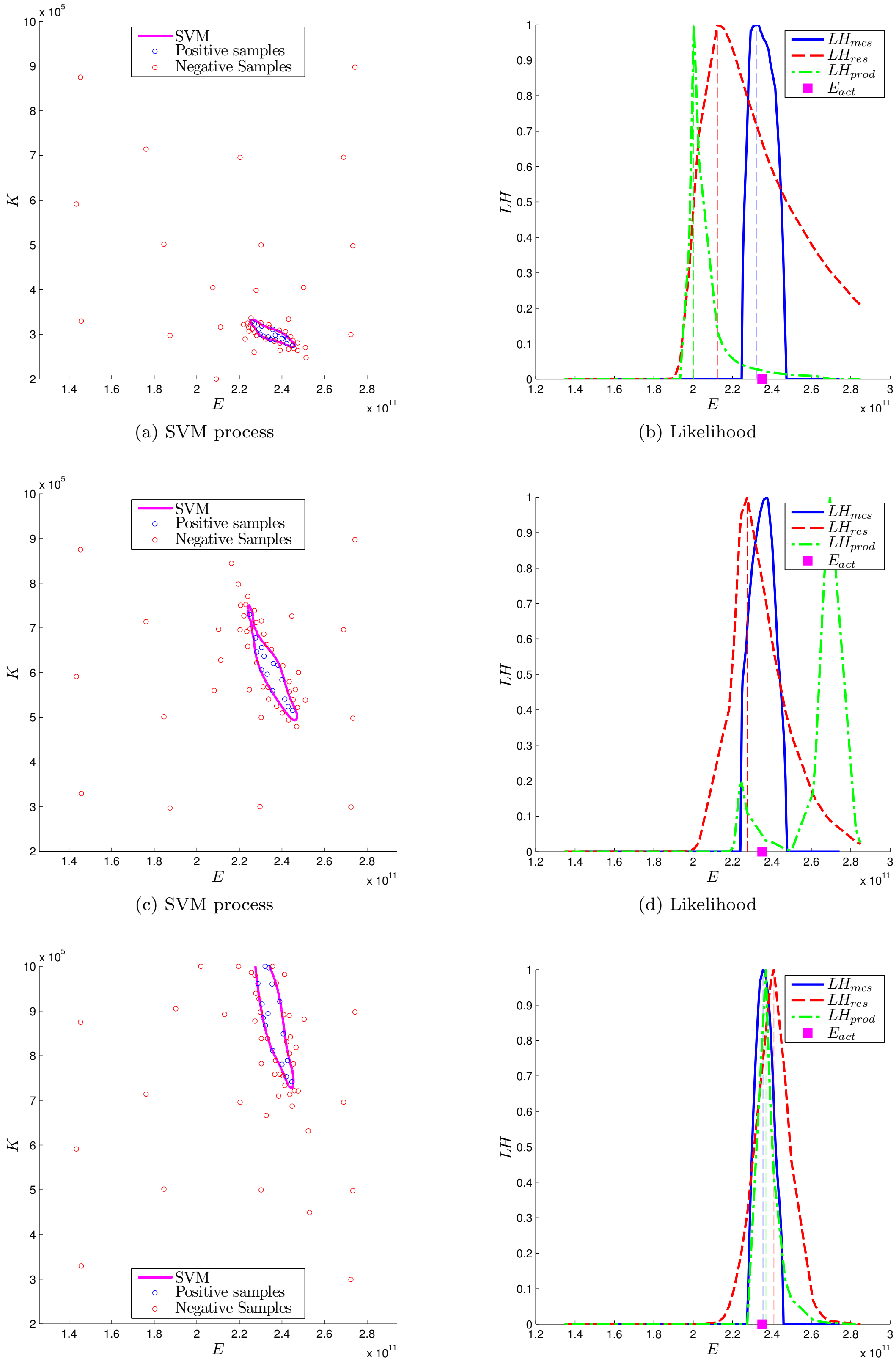

(a) SVM process (b) Likelihood

(c) SVM process (d) Likelihood

(e) SVM process (f) Likelihood

Figure 6: Results of the plate example for $E_{act} = 235 \times 10^9\ Pa$ and $K_{act} = 3 \times 10^5\ N.m^{-1}$ (a and b), $K_{act} = 6 \times 10^5\ N.m^{-1}$ (c and d) and $K_{act} = 9 \times 10^5\ N.m^{-1}$ (e and f). The figures on the left show the final SVM while the ones on the right show the likelihoods (S.I. units).

IV.B. Piano soundboard

A Finite Element model of a piano soundboard was implemented in ANSYS based on the characteristics of a 2.74 m Steinway piano. The model includes the soundboard with fourteen ribs running diagonally across the backside of the board in addition to two elevated curved bridges on the top of it, namely the bass bridge and the treble bridge (Figures 7a[a] and 7c[b]). Note that the model is exhaustively parametric and it can accommodate any piano geometry as well as any rib or bridge layout, including the number and the angle of the ribs. This model does not include down-bearing due to the strings[27] and crowning.[28] From a finite element point of view, the board is modeled with shell elements while the ribs and the bridge are modeled with beam elements (Figures 7b and 7d). In addition, the model is assumed linear with no stress stiffening. Note that, in general, stress stiffening and geometric nonlinearities might have an influence on the natural frequencies. However, this was not accounted in the proposed demonstrative example.

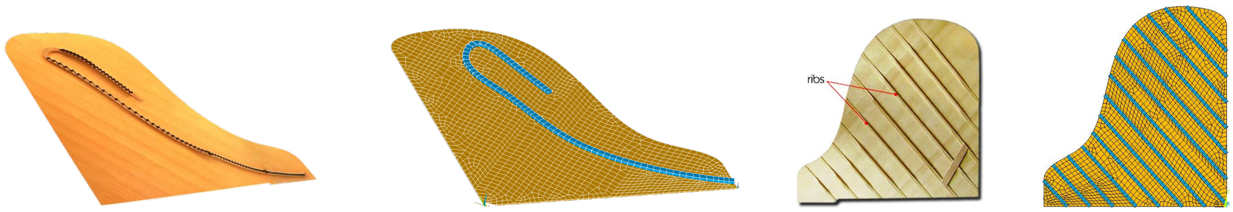

(a) Picture of the bridges[a] (b) FEM representation (c) Picture of the ribs[b] (d) FEM representation

Figure 7: Picture and fully parameterized Finite Element model of a piano soundboard. Upper face contains the bridges and the bottom face is stiffened with ribs.

Material properties of the wood, and their inherent variability, represent a crucial aspect of the modeling. Sitka spruce is the chosen wood when building the model which is an orthotropic material characterized by distinct properties in the longitudinal, and transverse directions. Note that bridges and stiffeners are assumed isotropic for simplicity. We wish to identify material properties such as the longitudinal Young's modulus and the wood density.

Among the difficulties to model a piano soundboard, the boundary conditions play a major role in its modal behavior. These boundaries replace the case of the piano which represents the attachment between the edges of case, the soundboard and the cast Iron plate (Figure 8[c]). For these reasons the soundboard is assumed to be clamped except for the out of plane translational degree of freedom. This degree of freedom is replaced by a translational spring stiffness K, as in the previous plate example. Two cases of model updating are considered: one where only the Young's modulus of the soundboard E is to be identified whereas the density of the soundboard ρ and the stiffness K of the springs are aleatory random variables (Table 3a). The second case is where both E and ρ are to be identified and only K is aleatory (Table 3b). It is noteworthy to mention that the SVM needs to be constructed only once and can then be re-used for various scenarios.

Figure 8: Global elements of a Steinway piano[c]. In the Finite Element Model, springs are used to simulate the link between the soundboard and the case.

For this example, fictitious measurements are obtained by running the model with the following values: $E_{act} = 11 \times 10^9\ Pa$, $\rho_{act} = 445\ Kg.m^{-3}$ and $K_{act} = 10^7\ N.m^{-1}$. The identification is based on the first five modes. The $\boldsymbol{\varepsilon}$ vector is set to:

$$\boldsymbol{\varepsilon} = \begin{bmatrix} 0.002 & 0.002 & 0.002 & 0.002 & 0.002 & 0.1 & 0.00002 \end{bmatrix}^T \tag{18}$$

where the 6^{th} (resp. 7^{th}) value is the restriction for all extra-diagonal MAC terms (resp. all diagonal MAC terms).

[a] pianotreasure.com
[b] www.piano.christophersmit.com
[c] einfotojedentag.blogspot.com

Table 3: Parameters for the two scenarios applied to the piano soundboard (S.I. units).

(a) Parameters used for the piano soundboard, case with one parameter to identify.

Deterministic	Epistemic	Aleatory	
numerous	E	ρ	K
numerous	N/a	$U(430, 450)$	$U(5 \times 10^6, 10^8)$

(b) Parameters used for the piano soundboard, case with two parameters to identify.

Deterministic	Epistemic		Aleatory
numerous	E	ρ	K
numerous	N/a	N/a	$U(5 \times 10^6, 10^8)$

The SVM is constructed using a 50 points CVT DOE and 200 adaptive sample points. The final SVM is depicted in Figure 9a. The likelihood obtained in the first case is displayed on Figure 9b. The MLE gives $E_{est} = 10.85 \times 10^9\ Pa$. The likelihood obtained in the second case is shown on Figure 9c. The MLE gives $E_{est} = 10.9 \times 10^9\ Pa$ and $\rho_{est} = 445.64\ Kg.m{-}3$. Recall that the computational cost is only 250 calls of the model. Nevertheless, the identified values are close to the actual ones.

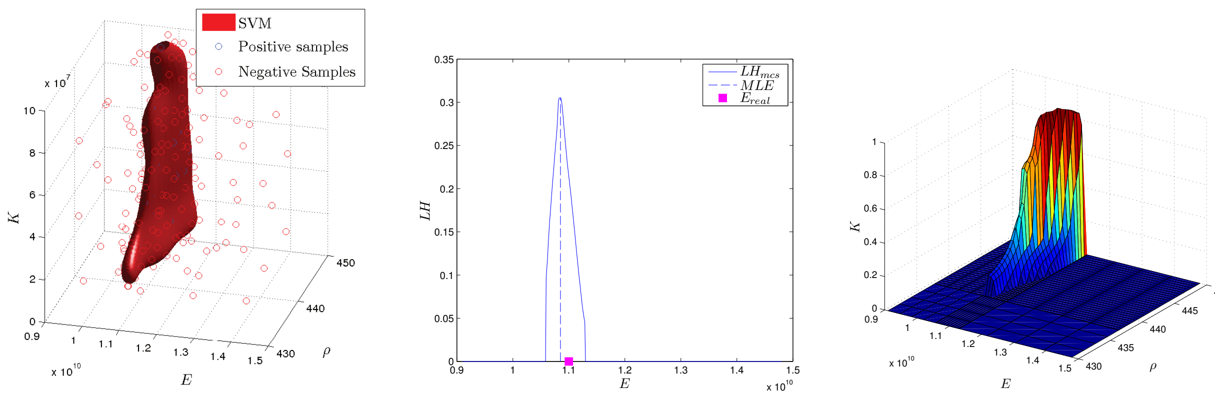

(a) SVM for the piano soundboard example.

(b) 1D likelihood for the piano soundboard example.

(c) 2D likelihood for the piano soundboard example.

Figure 9: Graphical results for the piano soundboard example.

V. Conclusion

An approach to perform model update using fidelity maps has been introduced. The construction of explicit fidelity maps, constructed using an SVM in a space with aleatory and epistemic uncertainties, allows one to efficiently calculate a likelihood with Monte-Carlo simulations. In order to obtain an accurate boundary and reduce the number of model calls, an adaptive sampling scheme is used. Because SVM is a classification method, a large number of model outputs, even correlated, can be used. Finally, this approach do not rely on any assumption, except a user define vector of variables, $\boldsymbol{\varepsilon}$.

The next steps of this research will involve an increase in the dimensionality of the problems solved in order to check the scalability of the approach. In addition, importance sampling will be used to improve the computation of the likelihood. Finally, the approach will be tested on a more realistic model of a piano soundboard with nonlinear behavior and actual experimental modal testing.

VI. Aknowledgments

Support from the National Science Foundation (award CMMI-1029257) is gratefully acknowledged. The authors would also like to thank Ms. Fatma Mokdad for her help in the construction of the Finite Element Model of the piano soundboard.

References

[1]Marwala, T., Mdlazi, L., and Sibisi, S., "Finite Element Model Updating Using Bayesian Approach," *Arxiv preprint arXiv:0705.2515*, 2007.

[2]Gogu, C., Haftka, C. G. R., Le Riche, R., J., M., and Vautrin, A., "Introduction to the Bayesian Approach Applied to Elastic Constants Identification," *AIAA Journal*, Vol. 48, No. 5, 2010, pp. 893–903.

[3]Nichols, J., Moore, E., and Murphy, K., "Bayesian identification of a cracked plate using a population-based Markov Chain Monte Carlo method," *Computers & Structures*, Vol. 89, 2011, pp. 1323–1332.

[4]Pratt, J., "FY Edgeworth and RA Fisher on the efficiency of maximum likelihood estimation," *The Annals of Statistics*, Vol. 4, No. 3, 1976, pp. 501–514.

[5]Aldrich, J., "RA Fisher and the making of maximum likelihood 1912-1922," *Statistical Science*, Vol. 12, No. 3, 1997, pp. 162–176.

[6]Press, S. and Press, J., *Bayesian statistics: principles, models, and applications*, Wiley New York, 1989.

[7]Carlin, B. and Louis, T., *Bayes and empirical Bayes methods for data analysis*, Vol. 7, Springer, 1997.

[8]Gunn, S., "Support vector machines for classification and regression," *ISIS technical report*, Vol. 14, 1998.

[9]Vapnik, V., *The nature of statistical learning theory*, Springer Verlag, 2000.

[10]Christianini, N. and Taylor, S., "An introduction to support vector machines (and othre kernel-based learning methods)," 2000.

[11]Schölkopf, B. and Smola, A., *Learning with kernels: Support vector machines, regularization, optimization, and beyond*, the MIT Press, 2002.

[12]Basudhar, A., Missoum, S., and Harrison Sanchez, A., "Limit state function identification using support vector machines for discontinuous responses and disjoint failure domains," *Probabilistic Engineering Mechanics*, Vol. 23, No. 1, 2008, pp. 1–11.

[13]Basudhar, A. and Missoum, S., "Adaptive explicit decision functions for probabilistic design and optimization using support vector machines," *Computers & Structures*, Vol. 86, No. 19-20, 2008, pp. 1904–1917.

[14]Basudhar, A. and Missoum, S., "An improved adaptive sampling scheme for the construction of explicit boundaries," *Structural and Multidisciplinary Optimization*, Vol. 42, No. 4, 2010, pp. 517–529.

[15]Kariya, T. and Kurata, H., *Generalized least squares*, Vol. 560, John Wiley & Sons Inc, 2004.

[16]Metropolis, N., Rosenbluth, A. W., Rosenbluth, M. N., and Teller, A. H., "Equation of State Calculations by Fast Computing Machines," *The Journal of Chemical Physics*, Vol. 21, No. 6, 1953, pp. 1087–1092.

[17]Hastings, W., "Monte Carlo sampling methods using Markov chains and their applications," *Biometrika*, Vol. 57, No. 1, 1970, pp. 97.

[18]Andrieu, C., De Freitas, N., A., D., and I., J. M., "An Introduction to MCMC for Machine Learning," *Machine Learning*, Vol. 50, 2003, pp. 5–43.

[19]Jaynes, E., "Prior probabilities," *Systems Science and Cybernetics, IEEE Transactions on*, Vol. 4, No. 3, 1968, pp. 227–241.

[20]Allemang, R., "The modal assurance criterion (MAC): twenty years of use and abuse," *Proceedings, International Modal Analysis Conference*, 2002.

[21]Marwala, T., *Finite Element Model Updating Using Computational Intelligence Techniques: Applications to Structural Dynamics*, Springer, 2010.

[22]Sacks, J., Welch, W., Mitchell, T., and Wynn, H., "Design and analysis of computer experiments," *Statistical science*, Vol. 4, No. 4, 1989, pp. 409–423.

[23]Jones, D., "A taxonomy of global optimization methods based on response surfaces," *Journal of Global Optimization*, Vol. 21, No. 4, 2001, pp. 345–383.

[24]Forrester, A. and Keane, A., "Recent advances in surrogate-based optimization," *Progress in Aerospace Sciences*, Vol. 45, No. 1-3, 2009, pp. 50–79.

[25]Basudhar, A., Dribusch, C., Lacaze, S., and Missoum, S., "Constrained efficient global optimization with support vector machines," *Structural and Multidisciplinary Optimization*, 2011, First Published Online, DOI: http://dx.doi.org/10.1007/s00158-011-0745-5.

[26]Bowman, A. and Azzalini, A., *Applied smoothing techniques for data analysis: the kernel approach with S-Plus illustrations*, Vol. 18, Oxford University Press, USA, 1997.

[27]Conklin Jr, H., "Design and tone in the mechanoacoustic piano. Part II. Piano structure," *The Journal of the Acoustical Society of America*, Vol. 100, 1996, pp. 695.

[28]Mamou-Mani, A., Frelat, J., and Besnainou, C., "Numerical simulation of a piano soundboard under downbearing," *The Journal of the Acoustical Society of America*, Vol. 123, 2008, pp. 2401.

A. Details about primary and secondary samples

This appendix provide further information about the equation and the motivations of the two adaptive samples used for EDSD. Although complete, this appendix is solely a summary of the work of Basudhar et al.[14]

A.A. Max-Min Sample

To refine the SVM, max-min samples are selected on the current SVM boundary at maximum distance to the closest neighbor training sample (Equation 19). A sample on the boundary has the highest probability of misclassification and compels the boundary to change. The selection of samples in sparsely populated regions avoids redundancy of data. Figure 10 shows the selection of a max-min sample and the SVM boundary update due to it.

$$\boldsymbol{x}_{mm} = \arg\max_{\boldsymbol{x}} \left(\min_i \|\boldsymbol{x} - \boldsymbol{x}_i\| \right), \quad \text{subject to:} \quad s(\boldsymbol{x}) = 0 \tag{19}$$

The objective function of this “max-min” problem (Equation 19) is non-differentiable, but it is made differentiable by reformulating with an additional variable z:

$$\boldsymbol{x}_{mm} = \arg\max_{\boldsymbol{x},z} z, \quad \text{subject to:} \quad \|\boldsymbol{x} - \boldsymbol{x}_i\| \geq z \quad \forall\, i = 1, ..., N, \quad s(\boldsymbol{x}) = 0 \tag{20}$$

In this work, the differentiable formulation of this global optimization problem is solved using a local optimizer (sequential quadratic programming) starting from multiple starting locations given by the existing training samples.

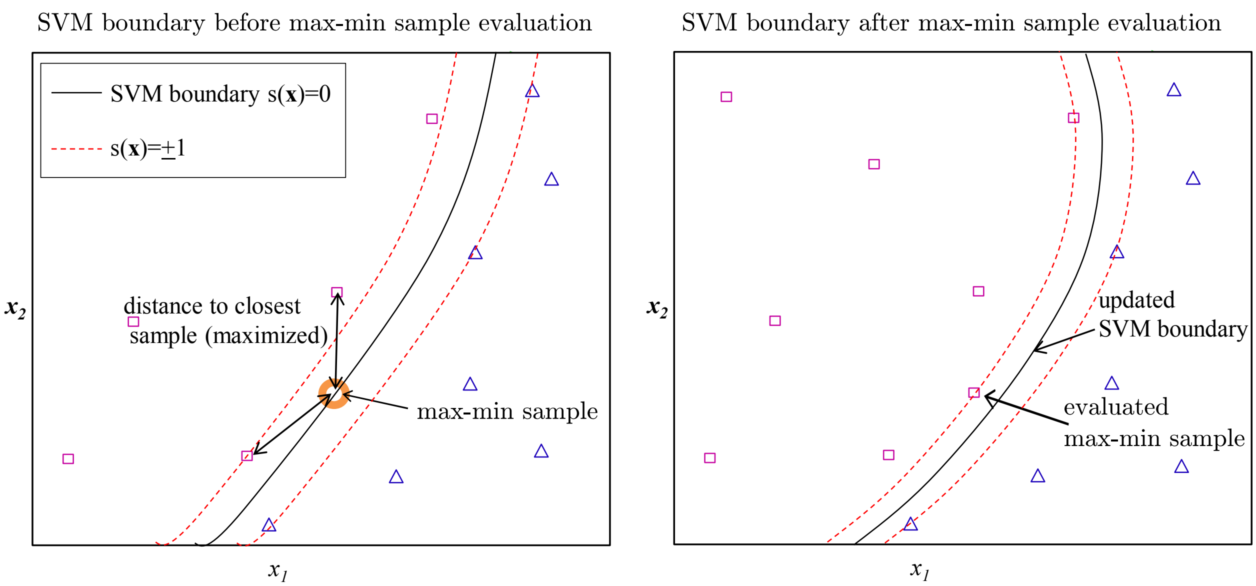

Figure 10: Selection of a new training sample on the SVM boundary while maximizing the distance to the closest sample. The right figure shows the updated SVM decision boundary.

A.B. Anti-Locking Sample

Although max-min samples always change the SVM, the change may be very small, which is referred to as “locking”. “Locked” parts of the SVM boundary are close to a training sample of one class, but far from any training sample of the other class (Figure 11). This situation is efficiently remedied by adding another training sample on the sparsely populated side of the boundary. The sample is placed close, but not on the current SVM boundary. Therefore evaluating an anti-locking sample either leads to a more balanced distribution of samples on both sides of the boundary or to a significant change in the SVM boundary (Figure 11).

Selection of the sample is a two step process: First locate $\boldsymbol{x}_b$, the point on the boundary for which Δd, the difference between the distance to the closest feasible sample $\boldsymbol{x}_c^-$ and the distance to the closest infeasible sample $\boldsymbol{x}_c^+$ is greatest:

$$\boldsymbol{x}_b = \arg\max_{\boldsymbol{x}} \left(\left\| \boldsymbol{x} - \boldsymbol{x}_c^- \right\| - \left\| \boldsymbol{x} - \boldsymbol{x}_c^+ \right\| \right), \quad \text{subject to:} \quad s(\boldsymbol{x}) = 0 \tag{21}$$

Next define a hypersphere with radius $R = 0.25 \cdot \Delta d$ centered at $\boldsymbol{x}_b$. The new anti-locking sample $\boldsymbol{x}_{al}$ is selected within the hypersphere by minimizing $s(\boldsymbol{x}_c)s(\boldsymbol{x})$, where $\boldsymbol{x}_c$ is the closest existing training sample. This essentially yields an anti-locking sample on the opposite side of the boundary to $\boldsymbol{x}_c$, at maximum distance to the boundary inside the hypersphere:

$$R = 0.25 \cdot \Delta d = 0.25 \cdot \left(\left\| \boldsymbol{x_b} - \boldsymbol{x}_c^- \right\| - \left\| \boldsymbol{x}_b - \boldsymbol{x}_c^+ \right\| \right) \tag{22}$$

$$\boldsymbol{x}_{al} = \arg\min_{\boldsymbol{x}} s(\boldsymbol{x})s(\boldsymbol{x}_c), \quad \text{subject to:} \quad \left\| \boldsymbol{x} - \boldsymbol{x}_b \right\| \leq R \tag{23}$$

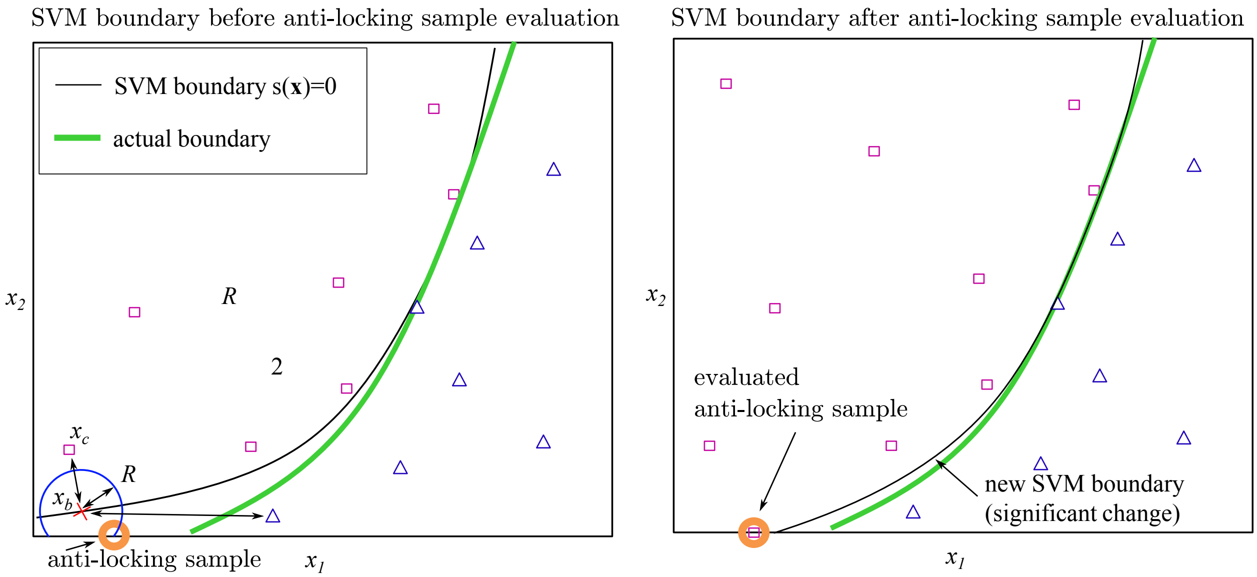

Figure 11: Evaluation of an anti-locking sample to prevent locking of the SVM boundary.

B. Product of the likelihoods and Residual

For comparison with the proposed approach, this appendix introduces two other methods to perform a scalable likelihood computation. These two approaches were used in the result section IV.

B.A. Product of the likelihood formulation

A widely used approach is to consider the likelihood as a product of “marginal” likelihoods. However this approach relies on a strong assumption (usually wrong) that the measurements are independent. The formulation of the product of the likelihood is straightforward:

$$\mathbf{e_{est}} = \mathbf{argmax}_{\mathbf{e}} \prod_{i=1}^{n_m} \mathbf{f}_{Y_i(\mathbf{E},\mathbf{A})|\mathbf{E}=\mathbf{e}}(y_i^{exp}) \tag{24}$$

The only appeal of this approach is that the “marginal” likelihoods can be computed as explained in Section B.C. In the case of costly models, surrogates such as Kriging[22–25] can be used for *each* individual measurement.

B.B. A Residual-Like method

For the sake of continuity with already existing methods, we derive a method based on a Residual. No claim is made about its efficiency, this approach is built to provide a comparison with the method introduced in III.B. The first idea is of course to define the Residual as:

$$r(\mathbf{e}, \mathbf{a}) = \sum_{i=1}^{n_m} (y_i^{exp} - y_i(\mathbf{e}, \mathbf{a}))^2 \tag{25}$$

However, it is usually a good idea to scale the different measurements as they can represent different quantities. A much more stable way to define the Residual is then to normalize the terms:

$$r(\mathbf{e}, \mathbf{a}) = \sum_{i=1}^{n_m} \left(\frac{y_i^{exp} - y_i(\mathbf{e}, \mathbf{a})}{y_i^{exp}} \right)^2 \tag{26}$$

It is then possible to define the estimated values as:

$$\mathbf{e_{est}} = \underset{\mathbf{e}}{\mathbf{argmax}}\ \mathbf{f}_{R(\mathbf{E},\mathbf{A})|\mathbf{E}=\mathbf{e}}(0) \tag{27}$$

It is noteworthy to mention that this method does not compute exactly the likelihood. This quantity can be computed as explained in Section B.C. It is noteworthy to mention that sometimes this approach and the product of the likelihoods formulation end up to be the same, if assuming only independent normal noises on the measurements.

B.C. Sequential uncertainty propagation

Constructing an empirical PDF (or joint) without presuming of its shape is a process that can usually only be done for low dimensionality. In this work, only PDFs of dimension 1 are computed, as described in Sections B.A and B.B. For each given $\mathbf{e^{(k)}}$, the uncertainties due to $\mathbf{A}$ are propagated and the probability density corresponding to the measurement is read. The process is shown on Figure 12 for e and y^{exp} scalar. Referring to the step where it is needed to fit the conditional PDF of Y in order to read the value at the measurement (the value of the likelihood for $e^{(k)}$), several ways are available in 1D or even for uncorrelated multidimensional one such as Gaussian mixture or kernel smoothing.[26] A general idea of Kernel Smoothing is depicted in Section B.D.

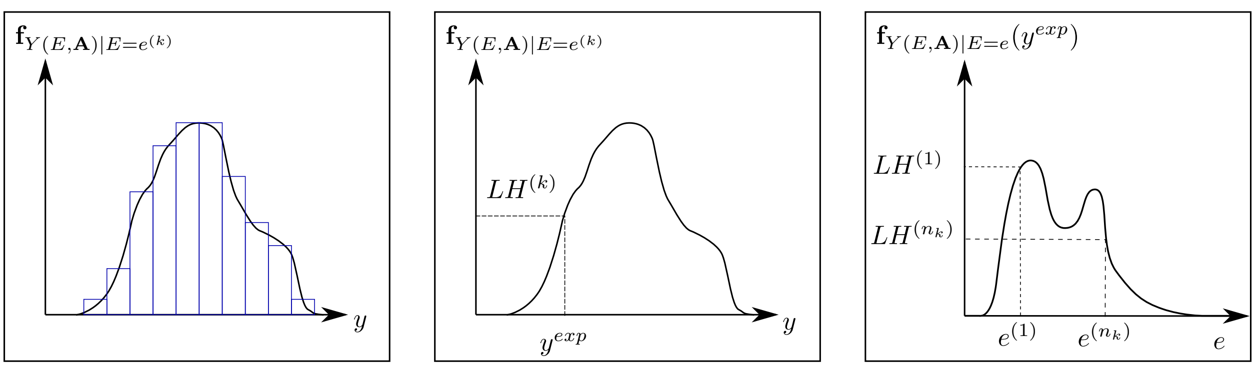

(a) For $c^{(k)}$, propagate the uncertainty through y, due to $\mathbf{U}$ and fit the PDF on top of it.

(b) Read the value of the conditional PDF for $y = y^m$ ($LH^{(k)}$).

(c) Repeat the process for $k = 1..n_k$ in order to construct the likelihood over the design space.

Figure 12: Description of the likelihood construction using sequential uncertainty propagation.

B.D. Kernel smoothing

Assuming the existence of a kernel $K(x)$ satisfying $\int K(x)dx = 1$ and symmetry about 0, for a set of point $\{x_1, \ldots, x_n\}$, $\mathbf{f}_X(x)$ can be estimated as:

$$\mathbf{f}_X(x) = \frac{1}{n}\sum_{i=1}^{n} K(x - x_i) \tag{28}$$

In fact, the kernel is often expressed as $K_h(x)$ where h is a parameter allowing to tune the kernel for better results. A basic illustration of this process is shown on Figure 13. For further informations, we refer the interested reader to.[26]

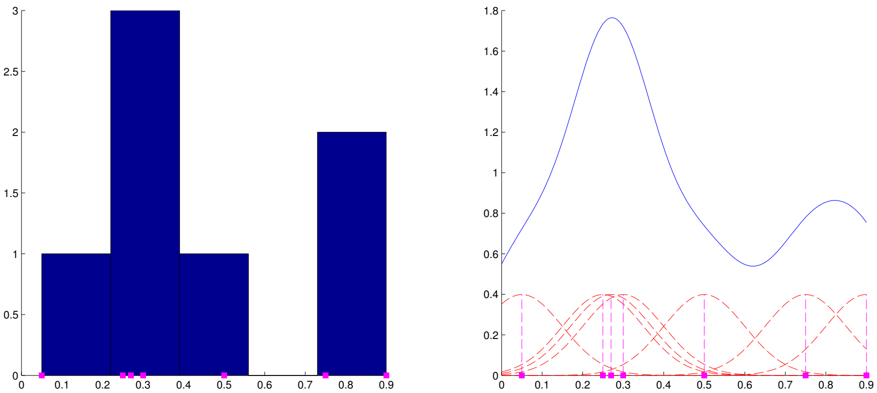

Figure 13: Basic illustration of the kernel smoothing density idea.